Supplementary Materials and Methods

Assay of ADP transport activity: specific conditions and kinetic scheme

The ADP-ATP exchange rate mediated by ANT1 was determined by measuring the time-dependent ADP concentrations using radioactive ^{14C}ADP and the inhibitor-stop method (1, 2) under the experimental conditions reported by Hashimoto (3). The measurement of ADP uptake in de-energized mitochondria in the presence of oligomycin minimizes the effects of adenine nucleotide metabolism and of membrane potential on the uptake. The endogenous ATP pool in mitochondria is preserved by the addition of the ATP synthase inhibitor oligomycin, which prevents both ADP phosphorylation (unlikely due to the lack of substrate) and ATP hydrolysis by the F1 subunit of the ATP synthase. Under these conditions and the low temperature (0°C) the exchange kinetics can be modelled by a first order equilibration between the externally added labeled ADP and the endogenously present (unlabeled) ATP. Given that the amount of ^{14C}ADP in the extramitochondrial compartment >> pool of endogenously present nucleotides, the equation describing ADP transport into mitochondria is (2):

$$\frac{d}{dt}[^{14C}ADP]_{ext}(t) = -\frac{v_T}{[^{14C}ADP]_{ext}(0)} * [^{14C}ADP]_{ext}(t)$$

v_T indicates the translocation activity in nmol per mg protein per minute. The solution for Δt=10 sec and $[^{14C}ADP]_{ext}$(t=0)=100 μMol is as follows:

$$\ln\left(\frac{[^{14C}ADP]_{ext}(t=10\,\text{sec})}{[^{14C}ADP]_{ext}(t=0\,\text{sec})}\right) = -\frac{v_T}{[^{14C}ADP]_{ext}(0)} * \Delta t$$

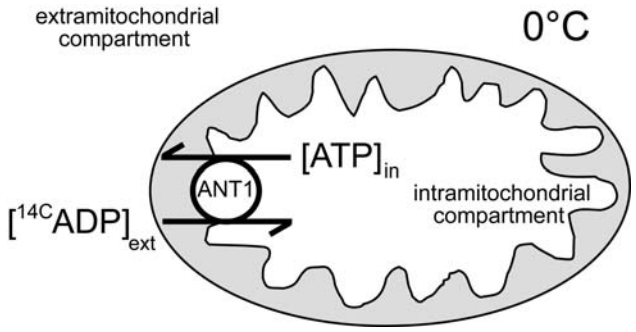

References

(1) Pfaff E, Klingenberg M. Adenine Nucleotide Translocation of Mitochondria. 1. Specificity and Control. Eur J Biochem 6: 66-79, 1968

(2) Pfaff E, Heldt HW, and Klingenberg M. Adenine Nucleotide Translocation of Mitochondria. Kinetics of the adenine nucleotide exchange. Eur J Biochem 10: 484-493, 1969

(3) Hashimoto M, Shinohara Y, Majima E, Hatanaka T, Yamazaki N, and Terada H. Expression of the bovine heart mitochondrial ADP/ATP carrier in yeast mitochondria: significantly enhanced expression by replacement of the N-terminal region of the bovine carrier by the corresponding regions of the yeast carriers. Biochim Biophys Acta 1409: 113-124, 1999

Supplementary Figure Legends

Supplementary Figure S1: Langendorff perfusion protocols

PreC: preconditioning with isoflurane (2.1 vol% for 15 min followed by 10 min of washout) prior to 40 min of test ischemia. ISCH: non-preconditioned hearts exposed to 40 min of ischemia. PreC+PP2: Src-FK inhibitor PP2 was co-administered with isoflurane.

Supplementary Figure S2: Characteristics of mitochondria from transformed yeast

Panel A: Mitochondrial size as assessed by flow cytometry (forward scatter). Panel B: Mitochondrial potential as measured by rhodamine 123 (Rh123) uptake. Yeast mitochondria expressing mutant adenine nucleotide translocase 1 (ANT1) exhibit significantly lower mitochondrial potential as evidenced by decreased uptake and quenching of Rh123 fluorescence. *P<0.01 vs $hANT1^{WT}$ (n=4).

Supplementary Figure S3: Src and Lck non-receptor tyrosine kinases can be found in rat heart mitochondria

20 μg of rat heart cytosolic and mitochondrial fractions were analyzed by Western blotting with antibodies against Src and Lck tyrosine kinases. The mitochondrial markers NADH dehydrogenase (ubiquinone) iron-sulfur protein 4 (NDUFS4), sarcomeric mitochondrial creatine kinase (sMtCK), adenine nucleotide translocase 1 (ANT1), and the cytosolic marker α-tubulin were used to identify cellular compartments.

Supplementary Figure S4: Structure of the bovine adenine nucleotide translocase 1 (ANT1; Protein Data Bank entry 1okc; http://www.pdb.org)

Panels A, B, C, G, and H: 3D structure representation of ANT1 with the tyrosine ladder (containing the two tyrosines Y190 and Y194) highlighted. Panel A illustrates the original configuration (WT). The residues Y194 and Y190 were subsequently exchanged with phenylalanine (Y194F and FF; panel B and panel C, respectively) to mimic the non-phosphorylated state. Panel G and panel H illustrate ANT1 structure with phosphorylated tyrosine residues pY194 and pY190. Panels D, E, F, I, and J: Corresponding electrostatic surface representations before (WT; panel D) and after site-directed mutagenesis to F (Y194F and FF; panel B and C, respectively) or addition of phosphate groups to Y194 (panel I) and to both Y190 and Y194 (panel J). Site mutations and post-translational modifications (phosphorylation) have been introduced in the original structural data using Discovery Studio® Software (Accelrys Inc., San Diego, USA). After minimizing the energy, electrostatic surfaces were

computed with the Adaptive Poisson–Boltzmann Solver. Positive and negative surfaces are shown in blue and red, respectively.

Supplementary Figure S5: Picture shows the distance between Y194 Cζ atom and K198 Nζ atom in different ANT1 forms. Reduced fluctuations in di-anionic pY194-ANT1 ($pY194^{2-}$) indicate salt bridge formation between Y194 and K198.

Supplementary Movie: Molecular dynamics simulation of the "tyrosine ladder"

The phosphate group of Y194 interacts with K198 potentially annihilating its putative interaction with D291. From left to right: $pY194^{-}$, $pY194^{2-}$, $pY190^{-}/pY194^{-}$, and $pY190^{2-}/pY194^{2-}$.

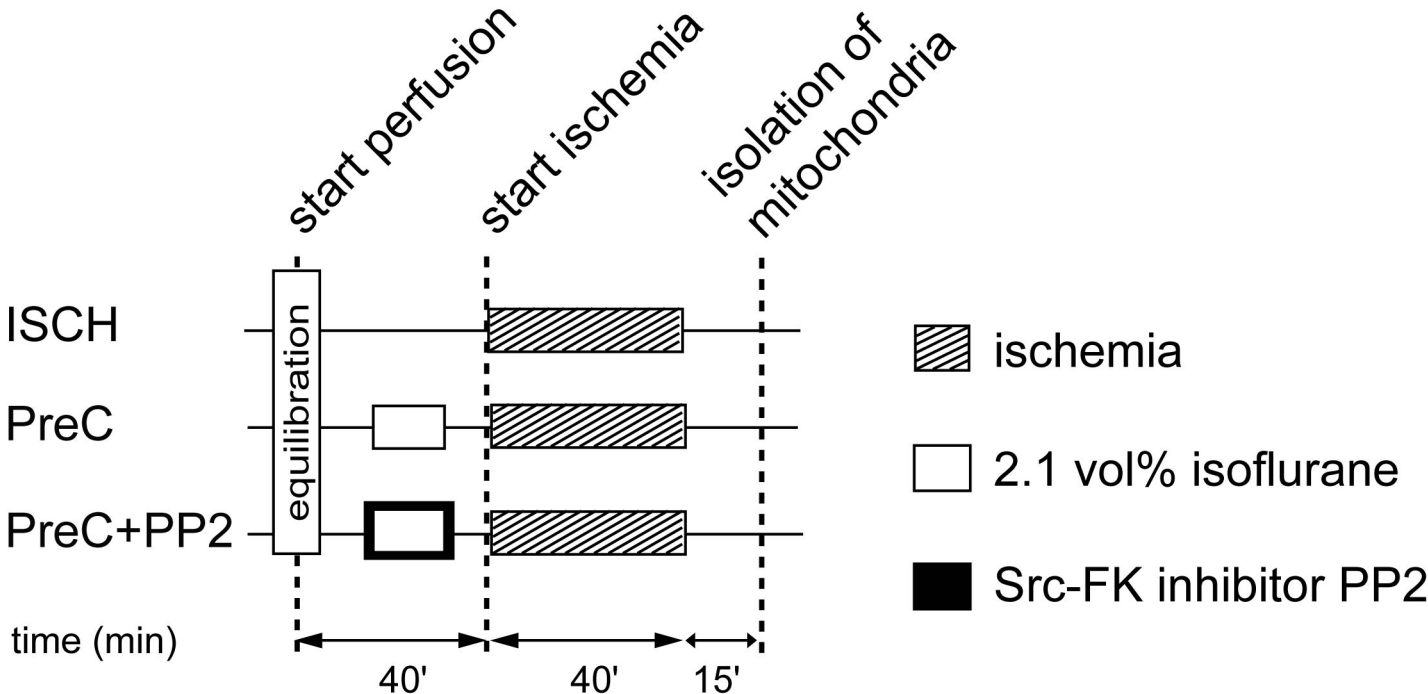
start perfusion
start ischemia
isolation of mitochondria
ISCH
PreC
PreC+PP2
equilibration
time (min)
40'
40'
15'
ischemia
2.1 vol% isoflurane
Src-FK inhibitor PP2

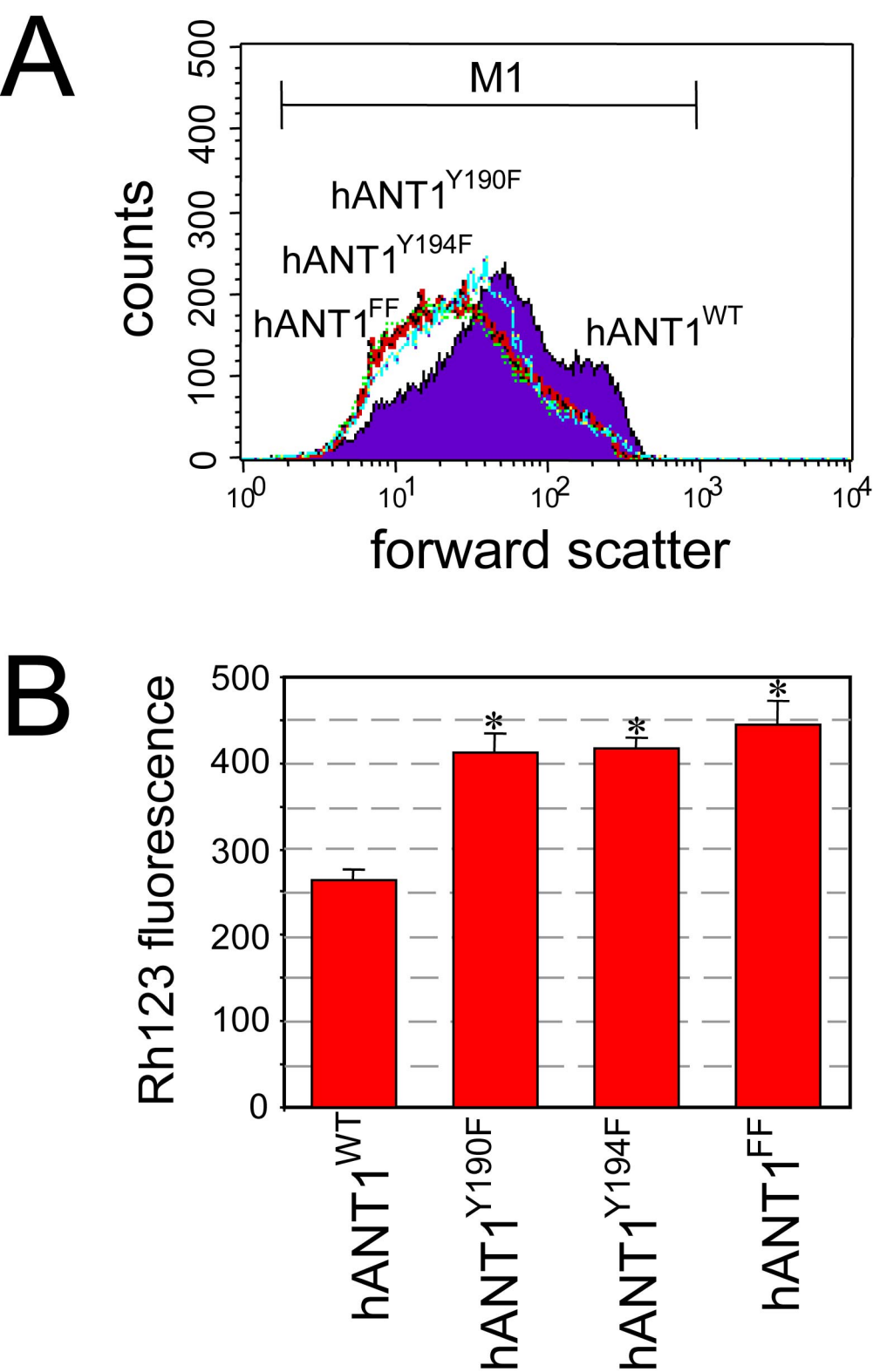
A
M1
hANT1Y190F
hANT1Y194F
hANT1FF
hANT1WT
counts
0
100
200
300
400
500
10^0
10^1
10^2
10^3
10^4
forward scatter
B
Rh123 fluorescence
0
100
200
300
400
500
*
*
*
hANT1WT
hANT1Y190F
hANT1Y194F
hANT1FF

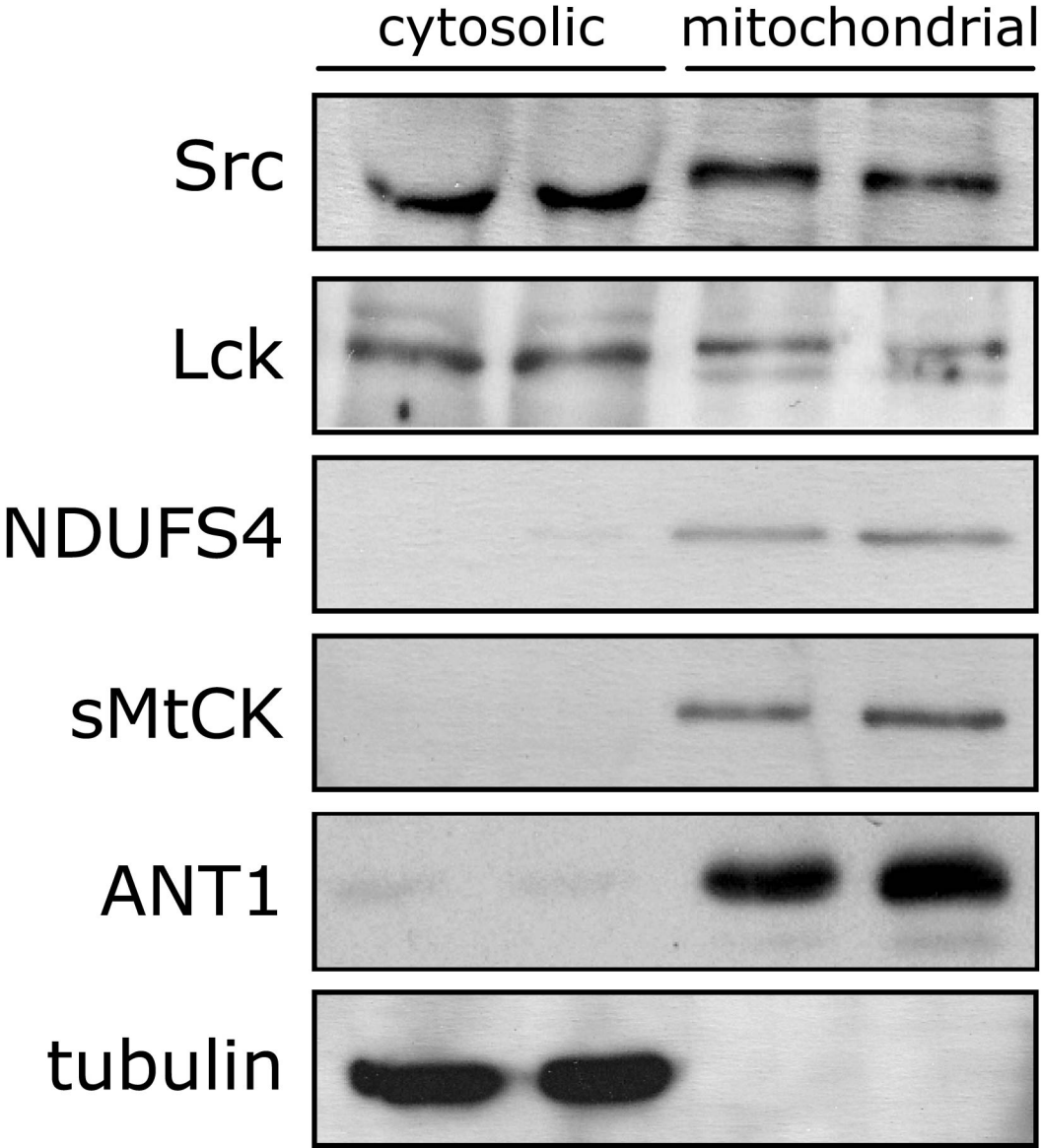
cytosolic
mitochondrial
Src
Lck
NDUFS4
sMtCK
ANT1
tubulin

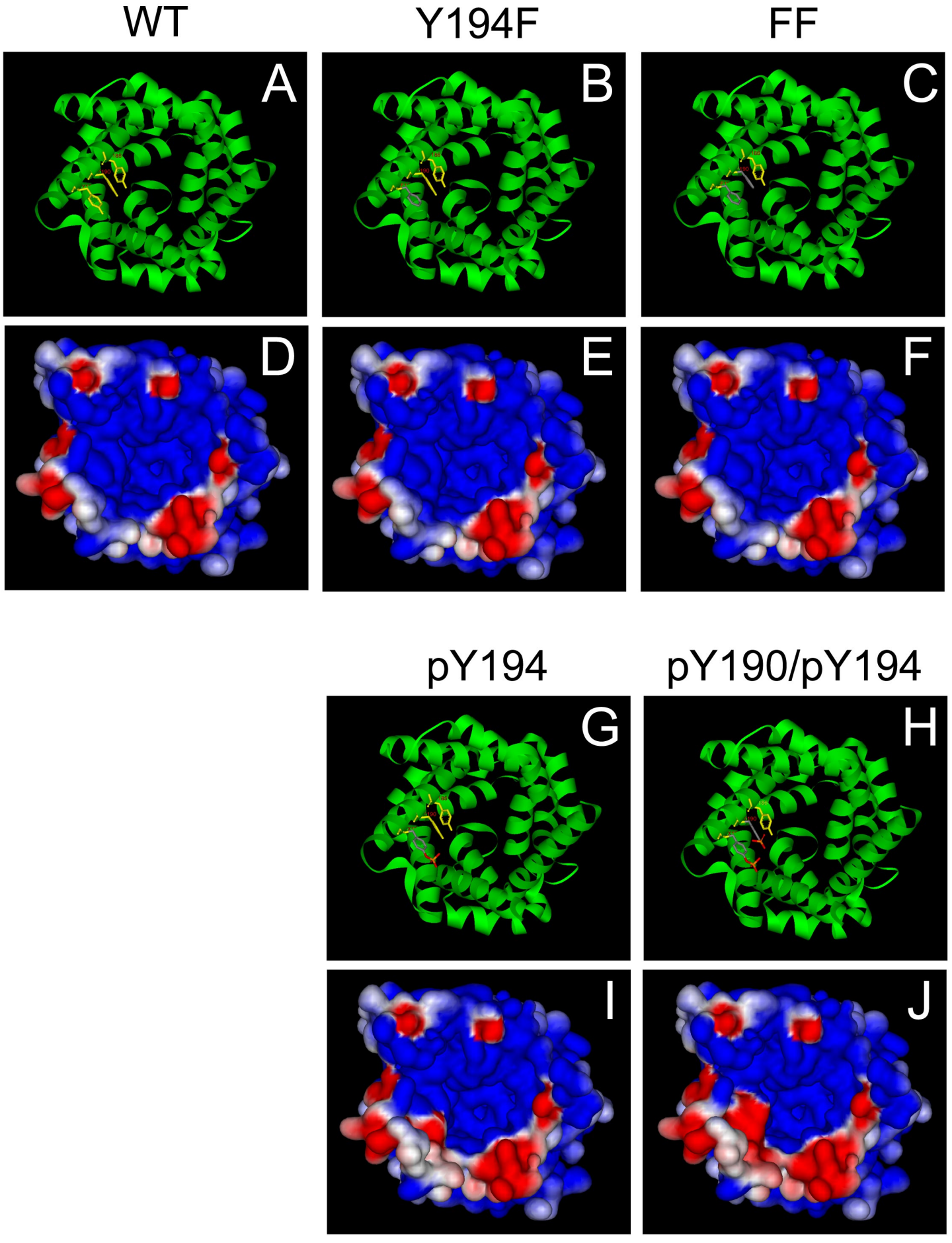
WT
Y194F
FF
A
B
C
D
E
F
pY194
pY190/pY194
G
H
I
J

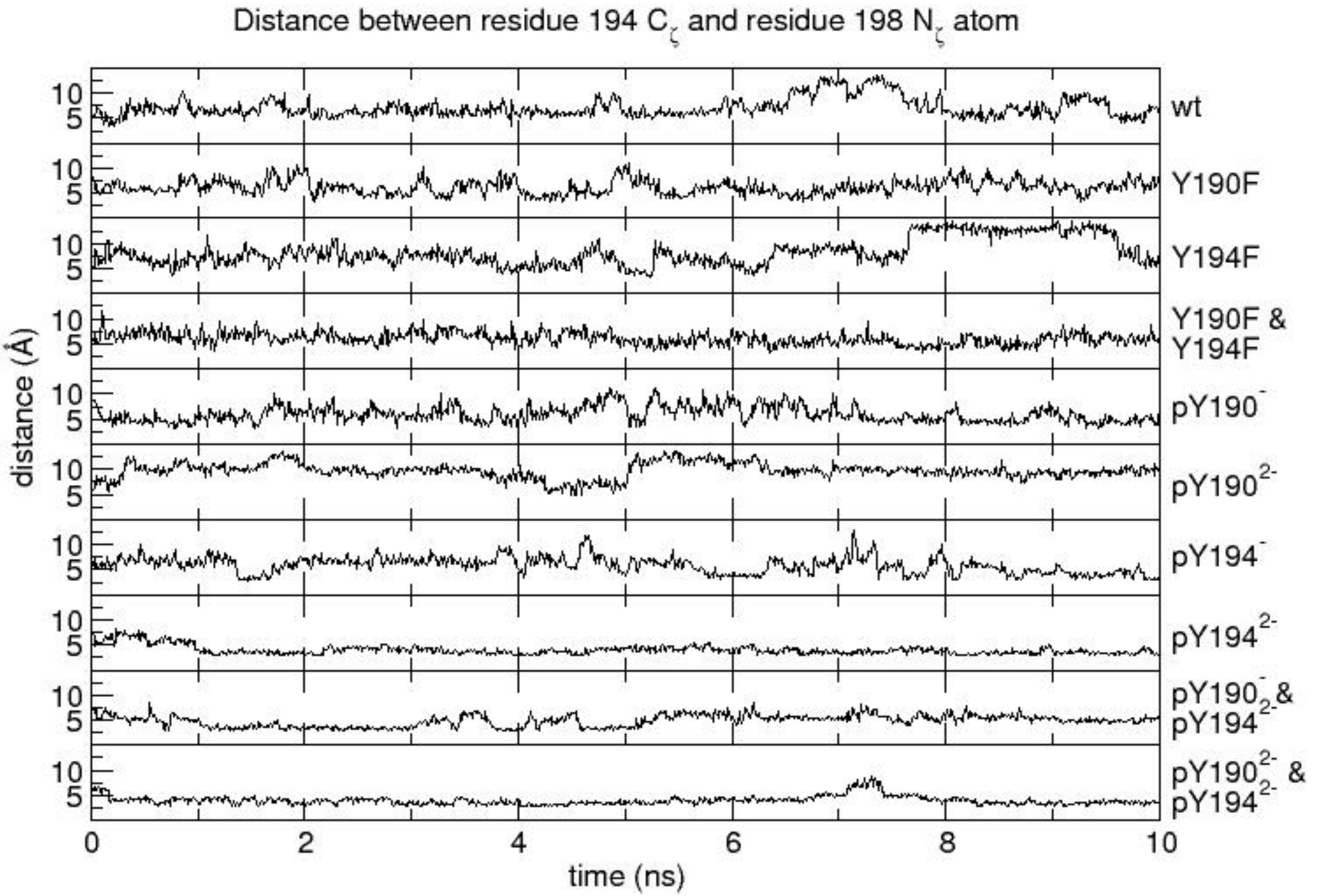
Distance between residue 194 C_ζ and residue 198 N_ζ atom
distance (Å)
10
5
wt
Y190F
Y194F
Y190F & Y194F
pY190$^-$
pY190^{2-}
pY194$^-$
pY194^{2-}
pY190$^-$ & pY194^{2-}
pY190^{2-} & pY194^{2-}
0
2
4
6
8
10
time (ns)